The Sugar Transporter family in wheat (*Triticum aestivum*. L): genome-wide identification, classification, and expression profiling during stress in seedlings

Hongzhan Liu[1,2], Chaoqiong Li[2], Lin Qiao[2], Lizong Hu[2], Xueqin Wang[2], Junsheng Wang[2], Xianle Ruan[2], Guangyu Yang[1], Guihong Yin[3,4], Chunping Wang[5], Zhongke Sun[2], Keshi Ma[2] and Lili Li[2,4]

[1] Zhoukou Academy of Agricultural Sciences, Zhoukou, Henan, China
[2] College of Life Science and Agronomy, Zhoukou Normal University, Zhoukou, Henan, China
[3] College of Agronomy, Henan Agricultural University, Zhengzhou, Henan, China
[4] Key Laboratory of Plant Genetics and Molecular Breeding, Zhoukou Normal University, Zhoukou, Henan, China
[5] College of Agronomy, Henan University of Science and Technology, Luoyang, Henan, China

ABSTRACT

The sugar transporter protein (STP) plays a crucial role in regulating plant growth and stress tolerance. We performed genome-wide identification and expression analysis of the STP gene family to investigate the STPSs' potential roles in the growth of wheat seedlings under stress. Here, a total of 81 TaSTP genes containing the Sugar_tr conserved motif were identified within the wheat genome. Bioinformatic studies including phylogenetic tree, chromosome position, and tandem repeat were performed to analyze the identified genes. The 81 TaSTP genes can be classified into five main groups according to their structural and phylogenetic features, with several subgroups, which were located separately on chromosomes A, B, and D. Moreover, six gene clusters were formed with more than three genes each. The results of three comparative syntenic maps of wheat associated with three representative species suggested that STP genes have strong relationships in monocots. qRT-PCR analysis confirmed that most TaSTP genes displayed different expression profiles after seedlings were subjected to six days of different stress (10% PEG6000, 150 mM NaCl, and their combination, respectively), suggesting that these genes may be involved in regulating plant growth and stress tolerance. In conclusion, 81 TaSTP genes were identified and their expressions changed under stress, indicating TaSTP's potential roles in wheat growth monosaccharide distribution is regulated.

Subjects Agricultural Science, Genomics, Molecular Biology, Plant Science
Keywords Wheat, Gene family, Sugar transporter, Syntenic maps, qRT-PCR

INTRODUCTION

Sugar is used as a universal energy source in higher land plants, playing important roles in cell development, signal transmission, and osmotic homeostasis under certain

abiotic stress conditions (*Lastdrager, Hanson & Smeekens, 2014*; *Rolland, Baena-Gonzalez & Sheen, 2006*). To date, it has been established that sugars produced by photosynthesis are distributed mainly as sucrose through the phloem to other parts of the plant. Sucrose is transported over long distances to the sink organs, some of which is unloaded directly to the sink organs via the symplast. Apoplastic sugar is the breakdown product of sucrose into glucose and fructose by sucrose invertase, and is taken in by transmembrane absorption mediated by sugar transporters (STP) before entering the sink cells (*Bush, 1999*; *Ludewig & Flügge, 2013*; *Paulsen, Custódio & Pedersen, 2019*). Sugar is typically transported across the plasma membrane or the vacuolar membrane by sugar transporters through active transport mechanisms or accelerated passive transport. In apoplastic loading, transmembrane transport is carried out by the sucrose transporter (SUT) or sugar carrier (SUC) in the plasma membrane (*Braun & Slewinski, 2009*). In the process of apoplastic unloading, invertase catalyzes the irreversible hydrolysis of sucrose into glucose and fructose, which is then unloaded by monosaccharide transporters (MST). Invertase and MST play a key role in this mode of transport. In sugarcane, eighty percent of the carbon fixed in leaves at midday is exported immediately (*Du et al., 2000*). Sucrose is the main form of long-distance carbohydrate transport in higher plants, while SUT, invertase, and MST are important in the loading and unloading of sugar molecules (*Slewinski, Meeley & Braun, 2009*; *Zhang, Zhang & Liu, 2015*; *Doidy, Vidal & Lemoine, 2019*). Sugar transport in plants is an important research topic and has economic implications (*Hedrich, Sauer & Neuhaus, 2015*). A key element for plant growth and development is the distribution of sugars between assimilate-exporting source tissues and sugar-consuming sink tissues; MST from the sugar transporter family contribute to the uptake of sugars into sink cells (*Rottmann et al., 2018*). More than 50 MSTs were identified in *Arabidopsis*. As a part of MST gene family, the STP subfamily is comprised of 14 monosaccharide/H+ symporters (*Schofield et al., 2009*). The STP subfamily encodes H$^+$-symporting monosaccharide transporters, which are able to transfer diverse hexoses (e.g., glucose, mannose) and/or pentoses (e.g., xylose) but not sucrose (*Rottmann et al., 2018*). Almost all STPs are a high affinity hexose transporter with specific expression in tissues, indicating that one of its main functions is to build up the sink required for photosynthate redistribution (*Büttner, 2007*; *Schofield et al., 2009*). This process plays a key role in maintaining source/sink characteristics and hormonal signals, as highlighted in the case of abiotic or biotic stresses (*Balibrea Lara et al., 2004*; *Roitsch & González, 2004*).

The plant STP protein commonly contains 12 structurally-conserved transmembrane domains (a large loop located in the cytoplasm in the middle of the sequence divides the whole protein into two parts; each contain six transmembrane domains) (*Bush, 1993*; *Yan, 2013*). Since the first STP gene was cloned from Chlorella (*Sauer & Tanner, 1989*), multiple STP genes have been identified by genome-wide identification with the rapid development of whole-genome sequences in various plants, such as *Arabidopsis* (*Büttner, 2010*), *Vitis vinifera* (*Afoufa-Bastien et al., 2010*), tomato (*Solanum lycopersicum*) (*Reuscher et al., 2014*), rice (*Oryza sativa*) (*Johnson & Thomas, 2007*), cassava (*Manihot esculenta*) (*Liu et al., 2018b*), *Zea mays* (*Kong et al., 2019*), pear (*Pyrus bretschneideri Rehd*) (*Li et al., 2015*), sweet oranges (*Citrus sinensis*) (*Zheng et al., 2014*), and rapeseed (*Brassica napus* L.) (*Zhang*

et al., 2020). In *Arabidopsis*, a total of 14 STP genes have been discovered to date, using a database search. These STP family genes exhibit different expression patterns and transport functions during plant growth and development and respond to stress processes (*Büttner, 2010*). For example, *AtSTP1* is reported to be abundant in seeds during imbibition and in seedling roots; moreover, transport by *AtSTP1* plays an important role in very high concentrations of exogenous sugar (*Sherson et al., 2010*). *AtSTP2* expression has been detected at the early stages of gametophyte development, specifically beginning at callose degradation and microspore release. Pollen-specific expression of *AtSTP6*, *AtSTP9* and *AtSTP11* has been shown during pollen germination and pollen tube growth (*Schneidereit, Scholz-Starke & Büttner, 2003*; *Scholz-Starke, Büttner & Sauer, 2003*; *Schneidereit et al., 2005*). Some reports have stated that AtSTP4 is mainly expressed in sink tissues such as roots and in mature leaves infected by fungi (*Endler et al., 2006*; *Fotopoulos et al., 2003*). Recent studies have shown that STP7 is highly expressed in tissues with cell wall transition, suggesting that STP7 may contribute to sugar uptake and is then recycling in the cell wall. STP8 and STP12 are highly expressed in the reproductive organs, and their protein products may contribute to the intake of sugar in the pollen tube and embryo (*Rottmann et al., 2018*).

In rice, the OsMST3 mRNA is detectable in leaf and roots (especially the sclerenchyma cells) as well as in the xylem in the root, which indicates that OsMST3 is involved in the accumulation of monosaccharides required for cell wall synthesis. Furthermore, STP genes also respond to stress from the environment, such as wounding or pathogen attack (*Liu et al., 2018b*). Moreover, drought stress has been reported to increase root length in the genotypes Gallagher, TAM111, and Yumar in wheat (*Djanaguiraman et al., 2019*).

Wheat is a globally important crop that supplies protein, vitamins, and minerals to humans. Wheat has a hexaploid A, B, and D genome (*Brenchley et al., 2012*). This species has a large 17 Gb genome, yet many STP genes remain undiscovered. STP genes play an important role in plant growth and development (*Mathieu et al., 2018*), so the identification of these gene families through genomic databases is important. We conducted an in-depth genome-wide analysis of the *TaSTP* gene family from the wheat genome (*International Wheat Genome Sequencing Consortium: IWGSC*) and included *TaSTP* gene models, genomic structures, phylogenetic relationships, chromosome locations, Ka/Ks ratios, and other bioinformatic analyses. Using qRT-PCR, we also analyzed the expression patterns of TaSTP genes in seedlings after 6 days of stress in NaCl, PEG6000, and NaCl+PEG6000. Our results will establish a solid foundation for further research on the functional roles of STP genes in wheat.

MATERIALS AND METHODS

Plant materials

The wheat cultivar Zhoumai 36 was germinated and grown in a tissue culture room at Zhoukou Normal University. The light conditions were set to dark for 12 h and light for 12 hours at 25–30 °C. Wheat seedlings were watered once every three days with Hoagland's nutrient solution. The stress treatment was performed when seedlings grew to the second-true leaf stage. Wheat seedlings were divided into four groups with 100 seedlings per group.

Seedlings from the first group to the third group were treated with 10% PEG6000 solution, 150 mmol L⁻¹NaCl, and 10% PEG6000 solution+150 mmol L⁻¹NaCl, respectively. The other group was left untreated as a control check (CK). Furthermore, different seedling tissues, such as leaves, stems, and roots, were collected to prepare the mixed cDNA template, which was used for *TaSTP* gene cloning. All fresh materials were quickly frozen in liquid nitrogen and stored in a −80 °C refrigerator for total RNA isolation.

Identification and characteristics of the TaSTP genes in wheat

The consensus protein sequences (PF00083) from the Sugar_tr hidden Markov model (HMM) were downloaded from Pfam 31.0 to identify the STP genes in wheat (https://pfam.xfam.org/family/PF00083). Then, the whole-genome data of wheat (*IWGSC*) and *Brachypodium distachyon* (BD) were obtained from the International Wheat Genome Sequencing Consortium and Phytozome v12.1 website. The HMM profile was used as a query to identify all STP-containing sequences in wheat and BD by searching against the downloaded genome with an *E*-value of <1e⁻⁵. Furthermore, all candidate TaSTPs were verified using Pfam and SMART (http://smart.embl-heidelberg.de/) to confirm that they contained the core domains. All potentially redundant TaSTP sequences and sequences lacking a part of STP domain or complete STP domain were discarded based on the sequence alignments generated by ClustalX software. Finally, a total of 81 STP protein sequences, which were encoded by 81 genes in the same subgroup as that in *Arabidopsis thaliana,* were identified in the wheat genome.

Phylogenetic analysis

For the phylogenetic tree of *TaSTP*, 14 *Arabidopsis* AtSTPs, eight rice STP protein sequences, six brachypodium distachyon STP protein sequences, eight foxtail millet STP protein sequences, 20 cassava STP protein sequences, 20 *Ricinus communis* STP protein sequences, and 81 full-length TaSTP protein sequences were aligned using ClustalX 2.1 (http://clustalx.software.informer.com/2.1/). A neighbour-joining (N-J) tree was constructed with the alignments using MEGA 7.0 software (*Kumar, Stecher & Tamura, 2016*) with bootstrap analysis from 1,000 replicates. The STP genes were named *TaSTP1* to *TaSTP81* according to their positions on the chromosomes.

Gene structure analysis and motif detection

The coding sequences (CDS) and genomic sequences of the STP genes were obtained from the International Wheat Genome Sequencing Consortium (http://plants.ensembl. org/Triticum_aestivum/Info/Index). By comparing the coding sequences and their chromosomal genomes, the exon-intron structures of the TaSTP family were generated using the Gene Structure Display Server website (http://gsds.gao-lab.org/). The MEME motifs of the predicted TaSTP proteins were identified using MEME suite 5.0.1 (http://meme-suite.org/tools/meme). Subsequently, these files were optimized using TBtools (*Chen et al., 2018*).

Homologous gene pairs and synteny analysis

The Ka/Ks ratios of gene pairs in duplication blocks were calculated using DnasP v6.0 and performed as described by *Cao et al. (2016)*. The parameters of the sliding window analysis

of the Ka/Ks ratios were set as follows: window size, 200 bp; step size, 25 bp. Moreover, TaSTP duplications were performed using the MCScanX program in the Bio-Linux system. In brief, with the BLAST outputs, the file of the gene positions, and the use of the MCScanX program, the TaSTP genes were classified into different types of duplications. We used Circos software to construct a schematic diagram (*Krzywinski et al., 2009*; *Liu et al., 2018b*) to exhibit the synteny relationship of the orthologous TaSTP genes obtained from wheat and other selected species. The syntenic analysis maps were constructed using the Dual Systeny Plotter software (https://github.com/CJ-Chen/TBtools).

Expression profiles of the TaSTP genes in the RNA-Seq data

Public transcriptome data were downloaded from the website http://www.wheat-expression.com/. Subsequently, all TPM data were log10 transformed, which was detailed in a previous study (*Yue et al., 2018*), and a heat map was created using TBtools.

Network interaction and GO analysis

The protein interaction network analysis of the TaSTPs was conducted using the STRING v10.5 database (http://www.string-db.org) based on the orthologous genes between *Arabidopsis* and wheat. GO analysis was conducted by GOToolBox (http://genome.crg.es/GOToolBox/) and visualized with Tbtools.

RNA isolation and validation analysis

Total RNA was extracted using the Trizol method (TriQuick Reagent, Solarbio, China), denatured in agarose gel (1%), and stained with SolarGelRed (Solarbio, China) to check the quality of the mixed RNA. The first-strand cDNAs were synthesized using a PrimeScript RT reagent kit (Takara Bio, Tokyo) according to the manufacturer's instructions and stored at −20 °C. Specific primers were designed using Beacon Designer software version 8.13 (Premier Biosoft International, Palo Alto, CA, USA) for the quantitative real-time polymerase chain reaction (qRT-PCR); the primer sequence details are provided in Table S1. Detailed information on the qRT-PCR protocol was described in a previous study (*Liu et al., 2018a*).

RESULTS

Identification of the STP gene family in wheat

To identify the STP family genes in wheat, the Sugar_tr HMM profile (Pfam: PF00083) was used as a query in a BlastP search against the wheat genome database (International Wheat Genome Sequencing Consortium: IWGSC). A total of 476 candidate TaSTP proteins were identified from the wheat genome with an *E*-value of $<1e^{-5}$. To identify the members of the TaSTP protein family, the proteins were checked for the presence of the Sugar_tr domain by the Pfam database (*Finn et al., 2010*) and the SMART database (*Letunic & Bork, 2018*). A total of 86 candidate STP proteins were discarded in this study because of a lack of a part of STP domain or complete STP domain. Finally, a total of 390 putative *TaSTP* genes were identified in the wheat genome through a HMMER analysis. A phylogenetic tree was constructed according to the protein sequences of 390 putative TaSTP and 14 AtSTP. The
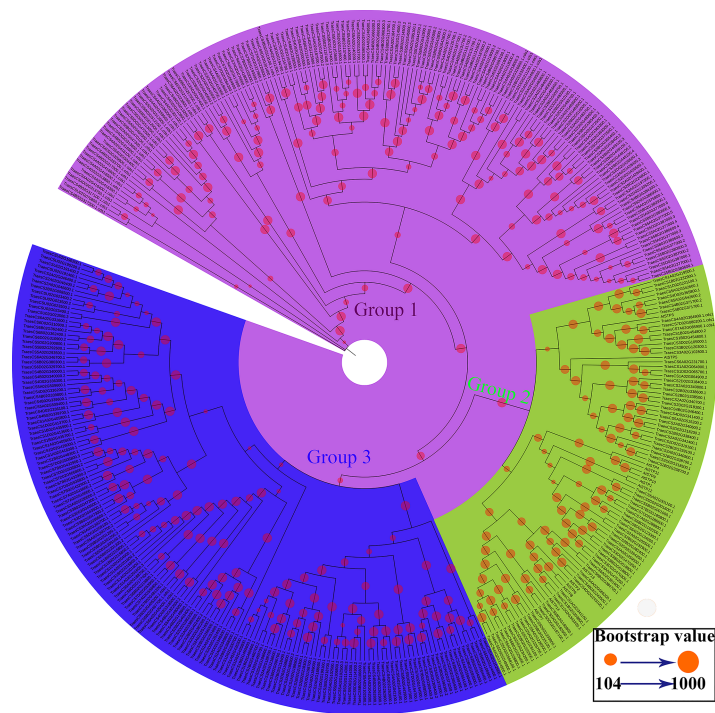
Figure 1 Phylogenetic relationships and subfamily designations of the STP proteins from wheat and *Arabidopsis thaliana*. An evolutionary tree was formed by the phylogenetic relationships of 390 predicted TaSTP proteins and *Arabidopsis thaliana* (*AtSTP1-AtSTP14*) proteins with 1,000 bootstrap replicates by MEGA v7.0. The subgroups containing STP proteins (*AtSTP1-AtSTP14*) from *Arabidopsis thaliana* are marked with green circle and black lines. There are 81 genes in wheat in the same group as that of *Arabidopsis thaliana*. The new names and accession numbers are shown in Table 1.

Full-size ☒ DOI: 10.7717/peerj.11371/fig-1

evolutionary tree was divided into three subgroups, and only the second subpopulation contains all *Arabidopsis* sugar transporters proteins, named AtSTP1 to AtSTP14 (Fig. 1, Group 2). These are all monosaccharide transporters and our focus was on the analysis of these monosaccharide transporters in wheat. There were 81 genes in wheat in the same group as in *Arabidopsis thaliana*. According to the position of the genes on the chromosomes, the 81 *TaSTP* genes were unevenly located on the wheat chromosomes and thus were named *TaSTP 1* to *TaSTP 81*. The general information on the 81 TaSTP members, including molecular weight, isoelectric point, CDS length, amino acid number, and transmembrane domain information, is summarized in Table 1. These genes were distributed on either the long or short arm of the A, B, and D chromosomes. Among them, chromosomes 1A, 2A, 3A, 4A, 5A, 6A and 7A had four, seven, two, three, eight, three, and two *TaSTPs*, respectively; chromosomes 1B to 7B had four, eight, three, four, five, two, and one TaSTPs, respectively; and chromosomes 1D to 7D had three, six, three, three, seven, one, and two *TaSTPs*, respectively (Table 1). We found that chromosomes A, B, and D had 29, 27, and 25 *TaSTP* genes, respectively. The open reading frames (ORFs) and the protein lengths of the *TaSTP* genes ranged from 1,080 to 1,848 bp in length and 359 to 615 amino acids in length, respectively (Table 1). The predicted molecular weights of the

Table 1 Information about the TaSTP genes in wheat.

Gene Name	Gene Locus	CDS Length (bp)	AA[a]	MW[b] (kDa)	pI[c]	TMD[d]
TaSTP1	TraesCS1A02G064900.1	1578	525	56.57	9.36	12
TaSTP2	TraesCS1A02G064900.2	1428	475	51.95	9.60	10
TaSTP3	TraesCS1A02G219500.1	1533	510	55.98	9.09	12
TaSTP4	TraesCS1A02G341100.1	1515	504	56.26	9.18	10
TaSTP5	TraesCS1B02G232900.1	1566	521	57.41	9.11	11
TaSTP6	TraesCS1B02G353800.1	1536	511	56.25	9.17	9
TaSTP7	TraesCS1B02G454800.1	1515	504	54.49	9.16	10
TaSTP8	TraesCS1B02G454800.2	1515	504	54.59	9.16	10
TaSTP9	TraesCS1D02G065700.1	1575	524	56.64	9.01	10
TaSTP10	TraesCS1D02G221100.1	1566	521	57.26	9.11	12
TaSTP11	TraesCS1D02G343200.1	1536	511	56.24	9.17	10
TaSTP12	TraesCS2A02G205500.1	1581	526	57.45	9.20	11
TaSTP13	TraesCS2A02G259500.1	1554	517	56.29	9.57	11
TaSTP14	TraesCS2A02G340600.1	1533	510	54.60	9.53	11
TaSTP15	TraesCS2A02G340700.1	1545	514	55.48	9.61	11
TaSTP16	TraesCS2A02G340800.1	1548	515	56.15	9.74	12
TaSTP17	TraesCS2A02G340900.1	1524	507	54.26	9.51	11
TaSTP18	TraesCS2A02G341400.1	1542	513	54.32	9.70	12
TaSTP19	TraesCS2B02G232900.1	1581	526	57.52	9.18	11
TaSTP20	TraesCS2B02G282400.1	1554	517	56.30	9.51	11
TaSTP21	TraesCS2B02G338400.1	1533	510	54.60	9.51	11
TaSTP22	TraesCS2B02G338500.1	1545	514	55.52	9.58	11
TaSTP23	TraesCS2B02G338600.1	1374	457	50.18	10.02	11
TaSTP24	TraesCS2B02G338700.1	1626	541	58.11	9.60	13
TaSTP25	TraesCS2B02G338700.2	1524	507	54.26	9.62	11
TaSTP26	TraesCS2B02G339100.1	1542	513	54.22	9.83	12
TaSTP27	TraesCS2D02G264200.1	1554	517	56.29	9.57	11
TaSTP28	TraesCS2D02G318200.1	1533	510	54.48	9.61	11
TaSTP29	TraesCS2D02G318300.1	1545	514	55.61	9.58	11
TaSTP30	TraesCS2D02G318400.1	1548	515	56.33	9.68	11
TaSTP31	TraesCS2D02G318500.1	1524	507	54.31	9.67	11
TaSTP32	TraesCS2D02G319100.1	1542	513	54.23	9.75	12
TaSTP33	TraesCS3A02G102800.1	1533	510	54.62	9.37	11
TaSTP34	TraesCS3A02G475200.1	1527	508	55.67	9.59	11
TaSTP35	TraesCS3B02G120300.1	1386	461	49.82	9.36	10
TaSTP36	TraesCS3B02G518800.1	1527	508	55.63	9.54	11
TaSTP37	TraesCS3B02G518900.1	1545	514	55.83	9.41	11
TaSTP38	TraesCS3D02G105000.1	1539	512	54.79	9.18	11
TaSTP39	TraesCS3D02G470200.1	1545	514	55.83	9.41	11
TaSTP40	TraesCS3D02G470300.1	1527	508	55.36	9.39	11
TaSTP41	TraesCS4A02G066200.1	1548	515	56.90	8.96	11

Table 1 (*continued*)

Gene Name	Gene Locus	CDS Length (bp)	AA[a]	MW[b] (kDa)	pI[c]	TMD[d]
TaSTP42	TraesCS4A02G314900.1	1545	514	55.93	9.28	12
TaSTP43	TraesCS4A02G384900.1.cds1	1542	513	54.28	9.84	12
TaSTP44	TraesCS4B02G243500.1	1545	514	56.69	8.95	11
TaSTP45	TraesCS4B02G346400.1	1554	517	55.01	9.92	10
TaSTP46	TraesCS4B02G371700.1	1575	524	57.00	8.99	11
TaSTP47	TraesCS4B02G371700.2	1848	615	67.04	8.59	11
TaSTP48	TraesCS4D02G243100.1	1545	514	56.70	8.95	11
TaSTP49	TraesCS4D02G341400.1	1548	515	54.87	10.05	10
TaSTP50	TraesCS4D02G365800.1	1581	526	57.24	9.06	11
TaSTP51	TraesCS5A02G001100.1	1551	516	56.28	9.33	11
TaSTP52	TraesCS5A02G182600.1	1590	529	57.47	9.07	12
TaSTP53	TraesCS5A02G226500.1	1566	521	56.55	9.26	11
TaSTP54	TraesCS5A02G226700.1	1563	520	56.30	9.06	12
TaSTP55	TraesCS5A02G226800.1	1587	528	57.29	8.79	12
TaSTP56	TraesCS5A02G515200.1	1548	515	54.99	9.98	10
TaSTP57	TraesCS5A02G542600.1	1158	385	41.27	9.79	8
TaSTP58	TraesCS5A02G542600.2	1581	526	57.26	8.98	11
TaSTP59	TraesCS5B02G001000.1	1554	517	56.05	9.16	11
TaSTP60	TraesCS5B02G180800.1	1587	528	57.43	8.86	10
TaSTP61	TraesCS5B02G225100.1	1563	520	56.39	9.34	11
TaSTP62	TraesCS5B02G225300.1	1542	513	55.76	9.05	10
TaSTP63	TraesCS5B02G225400.1	1587	528	57.27	8.78	12
TaSTP64	TraesCS5D02G001600.1	1554	517	56.21	9.27	11
TaSTP65	TraesCS5D02G187100.1	1590	529	57.45	8.97	10
TaSTP66	TraesCS5D02G233900.1	1563	520	56.47	9.26	11
TaSTP67	TraesCS5D02G234100.1	1563	520	56.44	9.23	12
TaSTP68	TraesCS5D02G234200.1	1587	528	57.31	8.90	12
TaSTP69	TraesCS5D02G549900.1	1545	514	55.95	9.20	12
TaSTP70	TraesCS5D02G558100.1	1515	504	55.16	9.62	11
TaSTP71	TraesCS6A02G134000.1	1572	523	57.27	8.57	12
TaSTP72	TraesCS6A02G231700.1	1530	509	55.08	8.90	12
TaSTP73	TraesCS6A02G351600.1	1080	359	39.55	10.05	6
TaSTP74	TraesCS6B02G162200.1	1572	523	57.41	8.43	11
TaSTP75	TraesCS6B02G384700.1	1578	525	58.34	8.81	11
TaSTP76	TraesCS6D02G123300.1	1572	523	57.27	8.42	12
TaSTP77	TraesCS7A02G085900.1.cds1	1545	514	54.45	9.89	10
TaSTP78	TraesCS7A02G288800.1	1536	511	55.38	8.44	12
TaSTP79	TraesCS7B02G185800.1	1536	511	55.33	8.59	12
TaSTP80	TraesCS7D02G080200.1.cds1	1539	512	54.12	9.92	12
TaSTP81	TraesCS7D02G286600.1	1536	511	55.37	8.64	12

Notes.
[a]Length of the amino acid sequence
[b]Molecular weight of the amino acid sequence
[c]Isoelectric point of the TaSTP
[d]Number of transmembrane domains, as predicted by the TMHMM server

TaSTPs ranged from 39.55 kDa to 67.04 kDa. The theoretical isoelectric points (pIs) of the *TaSTP* proteins ranged from 8.42 to 10.05. Moreover, 77 of the 81 TaSTPs contained 10 to 12 conserved transmembrane domains (TMDs), and most had 11 or 12; however, *TaSTP73*, *TaSTP57*, and *TaSTP6* carried only six, eight, and nine TMDs, and TaSTP24 carried 13 TMDs (Table 1).

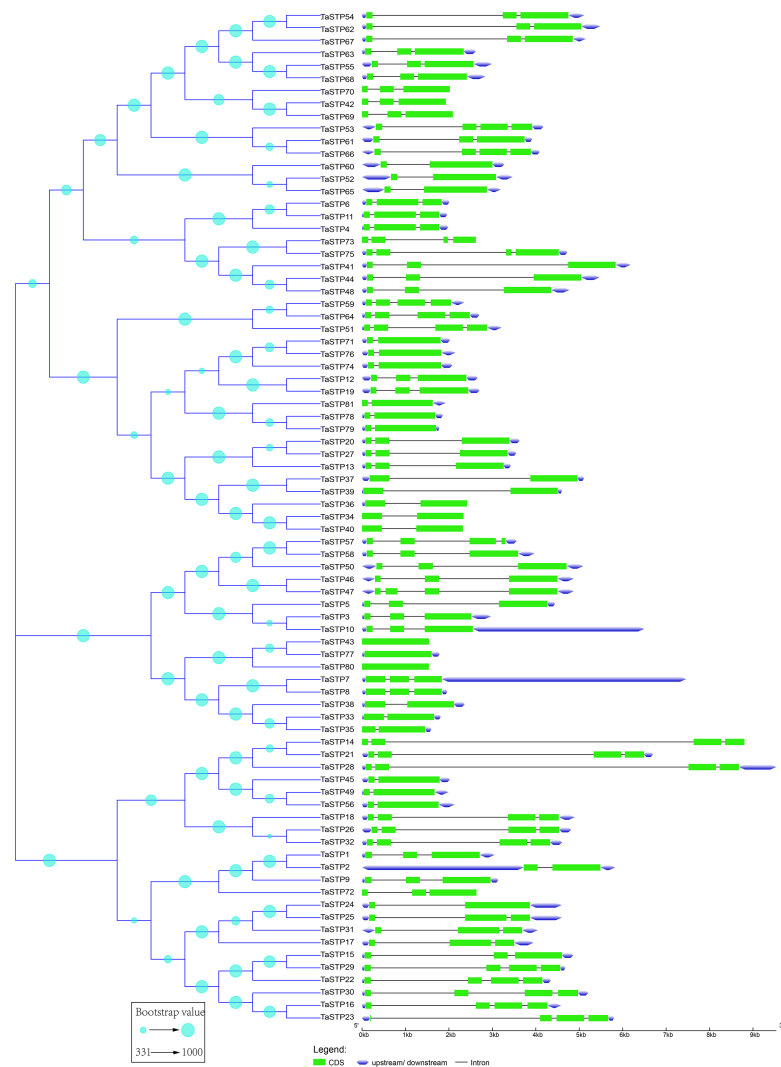## Sequence structure features of the *TaSTP* s

According to the neighbour-joining phylogenetic tree of the *TaSTP*s gene sequences, which was constructed using 1,000 bootstrap replicates by MEGA v7.0 (Pennsylvania State University, Philadelphia, PA, USA), the 81 *TaSTP* genes could be classified into three distinct groups according to the similarity of their gene sequences, and the bootstrap value ranged from 331 to 1,000 (Fig. 2). The largest group contained 42 *TaSTP* genes, and the other two groups contained 16 and 23 *TaSTP* genes, respectively. The *TaSTP* gene structures commonly had two, three, or four CDS divided by one, two, or three introns, except for *TaSTP43*, *TaSTP77,* and *TaSTP80* with one CDS. Furthermore, most of the TaSTP genes that were classified into the same subgroup exhibited similar gene structures, such as *TaSTP42,69* and *TaSTP70*, *TaSTP6,11* and *TaSTP4*, *TaSTP71,76*, and *TaSTP74* (Fig. 2).

To understand their functional regions, the conserved motifs of the TaSTP proteins were identified through the MEME website. Twenty motifs with minimum and maximum motif width set from six to 200 in the 81 proteins were analysed using the MEME tool. The results from MEME agreed with those from the phylogenetic tree (Fig. 3). It was found that most of the TaSTP proteins contained 15 or 16 motifs. *TaSTP2,15,22* and *29* had 14 motifs without motif 15 or another motif; *TaSTP23* and *TaSTP35* had 12 motifs without motifs six, eight, and 15; and *TaSTP73* had only nine motifs without motifs one, two, seven, nine, 14, and 15 (Fig. 3). We used Pfam to further analyze the 20 motifs and found that motifs one, two, three, five, and seven contained the Sugar_tr region. These five motif widths were 94, 72, 41, 36 and 45, respectively (Fig. 4, Table S2).

## Phylogenetic analysis of the TaSTP genes in seven species of mono-cotyledons and dicotyledons

To investigate the evolutionary relationships of the TaSTP gene family in monocotyledons of graminaceae (wheat, foxtail millet, brachypodium distachyon, and rice) and dicotyledons such as *Arabidopsis*, cassava, and *Ricinus communis*, we used the STP genes from wheat (81), brachypodium distachyon (6), foxtail millet (8), rice (8), cassava (20), *Ricinus communis* (20), and *Arabidopsis* (14) to construct a N-J phylogenetic tree usng MEGA 7.0 software with 1,000 bootstraps (Table S3). In the phylogenetic tree, we use different-colored clades to represent different species: wheat (black), brachypodium distachyon (gray), foxtail millet (green), rice (azure), *Arabidopsis* (red), cassava (blue), and Ricinus communis (purple). The results of the phylogenetic tree indicated that it can be roughly divided into five groups: Group I was one small branch with seven cloned wheat STP genes (*TaSTP3,5,10,46,47,57,58*), and the other large branch; Group II to Group V mainly contained the other genes, characterized by blue, purple, sky blue, and green areas,

Figure 2 Predicted TaSTP protein phylogeny and exon-intron structure. The exon–intron structures of the 81 TaSTP genes were generated by comparing the coding sequences and the corresponding genomic sequences using the GSDS website (http://gsds.gao-lab.org/) and optimized using TBtools. The construction method of the phylogenetic tree is the same as that of Fig. 1.

Full-size ⬇ DOI: 10.7717/peerj.11371/fig-2

respectively. The branches of Group II in the phylogenetic tree show that eight STP genes (*TaSTP7, 8, 33, 35, 38, 43, 77, 80*) and AtSTP3 were brought together. Group III consisted of twenty-three TaSTPs (*TaSTP1*, 2, 9, 14-18, 21-26, 28-32, 45, 49, 56, and 72), two RcSTPs, one MeSTP, BdMST1, AtSTP3 and SiMST1, and OsMST1 (Fig. 5). Nineteen TaSTPs (TaSTP*12, 13, 19, 20, 27, 34, 36, 37, 39, 40, 51, 59, 64, 71, 74, 76, 78, 79,* and *81*) clustered with six AtSTPs (AtSTP*1, 4, 9-12*), seven RcSTPs, five MeSTPs, four BdMSTs, and six SiMSTs in Group IV (Fig. 5). Group V consisted of twenty-three TaSTPs (TaSTP*4, 6, 9, 11, 41, 42, 44, 48, 52-55, 60-63, 65, 66-70, 73,* and *75*), six AtSTPs (AtSTP*2, 6, 7, 8, 13,* and *14*), twelve MeSTPs, ten RcSTPs, BdMST*4*, SiMST*4*, and OsMST*4* (Fig. 5).
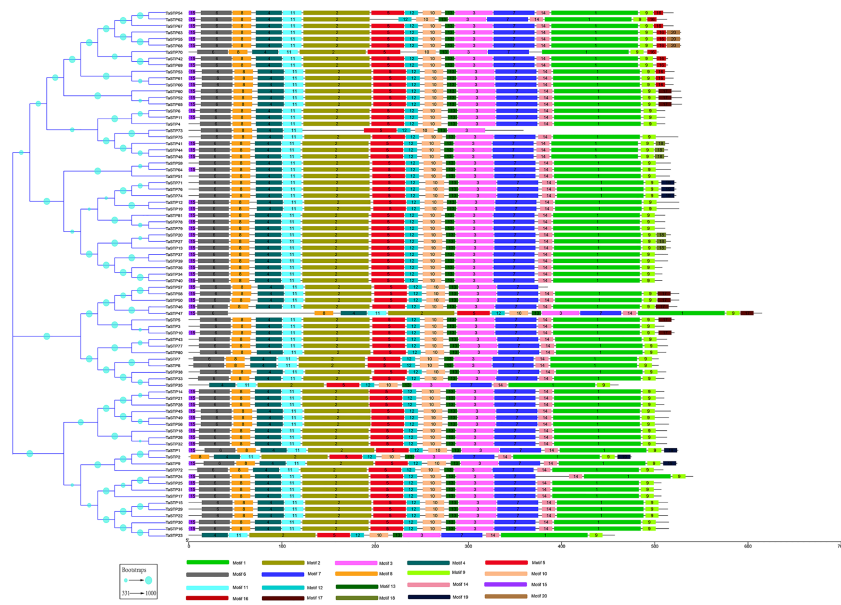
Figure 3 **MEME motif search results of the predicted TaSTP proteins by MEME suite 5.0.1.** The non-conserved sequences are shown by black lines, and the different motifs are represented by different coloured boxes numbered at the centre of the box and bottom of the figure. In addition, the lengths of the motifs in each protein are proportional. The phylogenetic tree is the same as that in Fig. 2.

Full-size 🖼 DOI: 10.7717/peerj.11371/fig-3
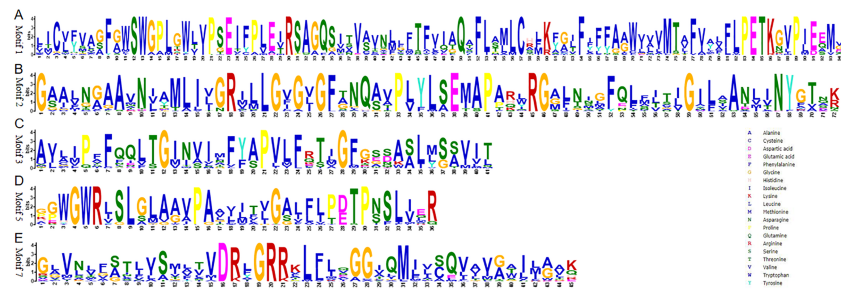
Figure 4 **Conserved motifs of Sugar_tr in STP proteins.** The motif logos and the amino acid compositions of the Sugar_tr motifs are as follows: Motif 1, Motif 2, Motif 3, Motif 5 and Motif 7. The *x*-axis represents the amino acid type and position. The *y*-axis shows the overall height of the amino acid stacks, which indicates the sequence conservation at a given position, while the height of the individual symbols within a stack indicates the relative frequency of a nucleotide base at that position.

Full-size 🖼 DOI: 10.7717/peerj.11371/fig-4

Chromosome location and gene duplication analysis

The approximate locations of the TaSTP genes on the chromosomes of wheat were determined by MapDraw software according to http://plants.ensembl.org/Triticum_aestivum/Info/Index. We found that the 81 genes were located separately on chromosomes A, B, and D. Moreover, *TaSTP14-TaSTP18*, *TaSTP21-TaSTP26*, *TaSTP28-TaSTP32*, *TaSTP53-TaSTP55*, *TaSTP61-TaSTP63*, and *TaSTP66-TaSTP68* formed a gene cluster with more than three genes on chromosomes 2A, 2B, 2D, 5A, 5B, and 5D, respectively (Fig. 6). We also investigated the tandem duplications and whole-genome duplications of
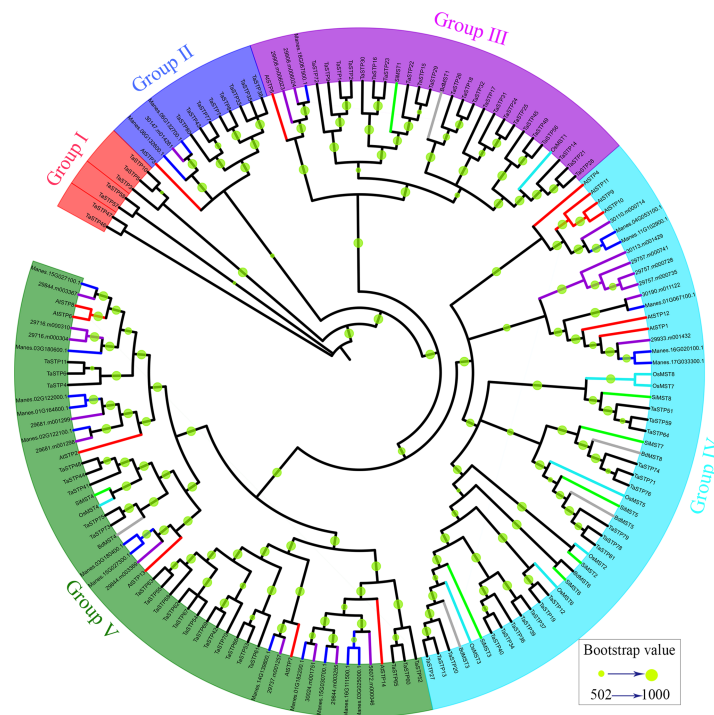
Figure 5 **Phylogenetic relationship of the TaSTP proteins in seven plant species.** The evolutionary relationship is presented using a phylogenetic tree. Five groups, which are named Group I to Group V are marked with diffirent lines. The bootstrap values of 502 to 1,000 are represented by the size of the green circles.

Full-size ☑ DOI: 10.7717/peerj.11371/fig-5

the 81 TaSTP genes. As shown in Fig. 6, the TaSTP genes were differentially distributed on 21 wheat chromosomes. Among these TaSTP genes, 159 pairs of genes exhibited whole-genome duplications/segmental duplications (Table S4). A total of 22, 23, and 21 TaSTP genes were distributed in the A, B and D sub-genome, respectively (B¿A¿D) as shown with the tandem replication events of multiple genes in Fig. 7. Initial gene loss likely occurred in the A genomes following tetraploidy and D genomes following hexaploidy to decrease functional redundancy and define the core wheat genes. There were nine, eleven, eight, nine, eighteen, six, and give genes in groups one through seven of the chromosomes, which showed three obvious gradients between groups two and five, and one, three, four and the other two groups. Specifically, chromosomes 5A, 5B and 5D had six, five, and seven genes, respectively, whereas chromosome 7B had only one TaSTP gene. These results indicated that the distribution of the TaSTP genes was not random in chromosomes and that gene replication events might have occurred in chromosomes two and five and may involve gene functions.

We constructed three comparative syntenic maps of wheat associated with three representative species, including rice, foxtail millet, and brachypodium distachyum to further infer the phylogenetic mechanisms of the wheat TaSTP family. A total of 25 orthologous TaSTP gene pairs were found between wheat and rice and brachypodium distachyum (Table S5; Fig. 8A). These TaSTP genes were found to be associated with at
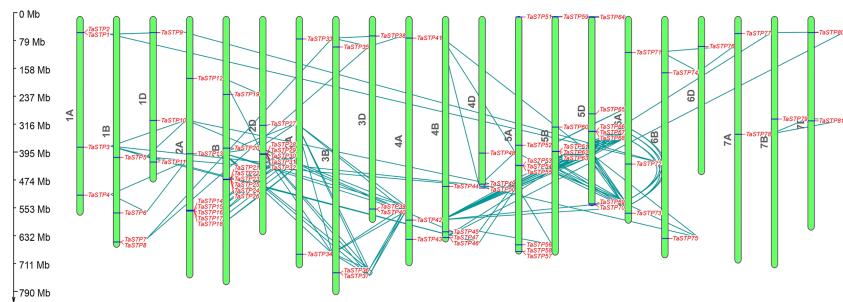
Figure 6 Chromosomal locations of the wheat sugar transporter (TaSTP) genes. Distribution of the TaSTP genes on the wheat chromosomes according to the linkage map. Tandem duplicates are connected by dark cyan coloured lines. In total, 81 TaSTP genes were mapped to 21 chromosomes (1A-7A, 1B-7B and 1D-7D). The scale is in bp (base pair). A total of six gene clusters containing three or more than three genes were distributed on the 2A, 2B, 2D, 5A, 5B, and 5D chromosomes, respectively.

Full-size 🖾 DOI: 10.7717/peerj.11371/fig-6
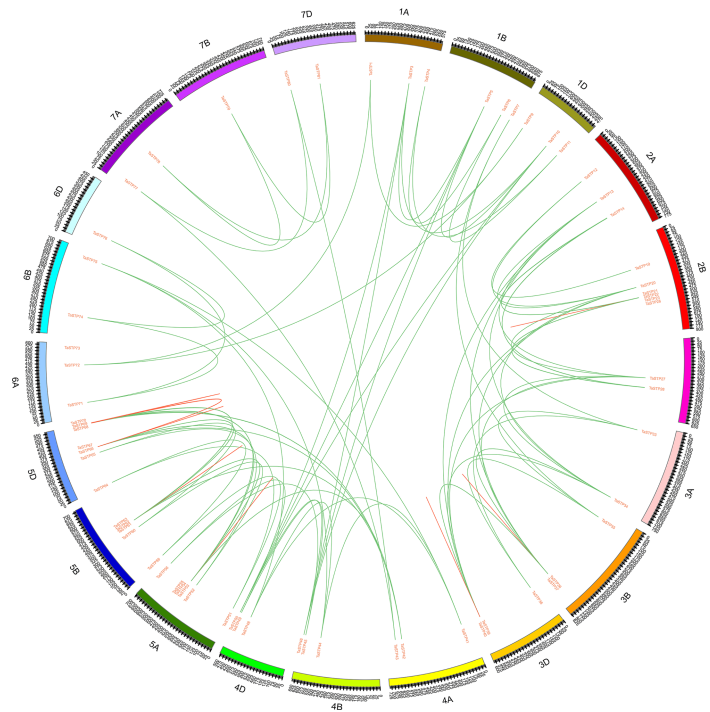
Figure 7 Localization and synteny of the TaSTP genes in the wheat genome. The TaSTP genes in wheat (TaSTP) were mapped to different chromosomes. The chromosome number is indicated on the outside. The numbers along the chromosome boxes represent sequence lengths in megabases. Gene pairs with a syntenic relationship are joined by a green line. The duplicated genes are joined by a red line.

Full-size 🖾 DOI: 10.7717/peerj.11371/fig-7

least three syntenic gene pairs (particularly between rice and brachypodium distachyum genes), such as *TaSTP12*, *TaSTP4,1* and *TaSTP48* (shown as different color lines in the figure). These genes may have played an important role in the STP gene family during evolution. Moreover, 38 orthologous TaSTP gene pairs were found between wheat and foxtail millet (Table S5; Fig. 8B). We calculated the Ka/Ks ratios of the STP gene pairs to
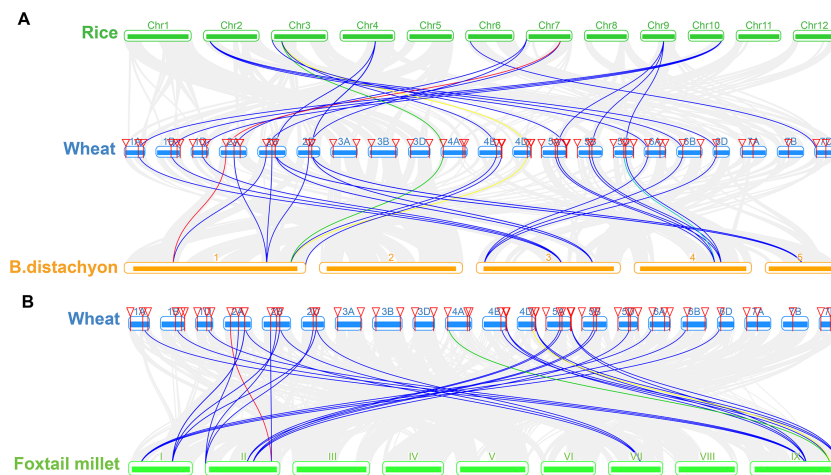
Figure 8 **Synteny analysis of TaSTP genes between wheat and three representative plant species.**
Gray lines in the background indicate the collinear blocks within wheat and other plant genomes, while
the other color lines highlight the syntenic TaSTP gene pairs. The specie names 'Wheat', 'Rice', 'B.
distachyon', and 'Foxtail millet' indicate *Triticum aestivum*, *Oryza sativa*, *Brachypodium distachyum* and
Setaria italica, respectively. (A) Synteny analysis of TaSTP genes between wheat and rice and *B. distachyon*;
(B) Synteny analysis of TaSTP genes between wheat and foxtail millet.

Full-size 🖼 DOI: 10.7717/peerj.11371/fig-8

better understand the evolutionary constraints acting on STP gene family. All orthologous
STP gene pairs had Ka/Ks < 1, suggesting that the wheat STP gene family might have
experienced strong purifying selective pressure during evolution (Table S6). These results
suggested that the STP genes of monocot have strong relationships.

Strong purifying selection for the TaSTP gene pairs in wheat

In general, a nonsynonymous (Ka)/synonymous (Ks) ratio > 1 indicates positive selection,
Ka/Ks ¡ 1 indicates purifying selection with functional constraints, and Ka/Ks = 1 indicates
neutral selection. In our study, the Ka/Ks ratios of most of the TaSTP paralogous pairs
were less than 1, and the ratio of only 1 paralogous pair was more than 1, namely, *TaSTP1
& TaSTP72*. Remarkably, of these Ka/Ks ratios <1, 147 TaSTP paralogous pairs were less
than 0.27 and appeared to be under strong purifying selection, 11 were between 0.27 and
0.98 and appeared to be under purifying selection, and one appeared to be under positive
selection (Fig. 9, Table S6).

Expression profiles of the TaSTP genes

The RNA-seq data from http://www.wheat-expression.com/ were used to explore the
expression profiles of the TaSTP genes in different tissues and under different abiotic
stresses. According to the heat map results, the expression level of 76 TaSTP genes (genes
with the same transcript were deleted) could be classified into A (yellow), B (blue), and
C (pale red) pattern groups (Fig. S1). In the pattern group A (yellow), most genes in the
different tissues showed low or no expression, and the genes *TaSTP28*, *TaSTP21*, *TaSTP1*,
TaSTP68, *TaSTP55*, and *TaSTP63* were expressed in the roots of Chinese spring wheat.
In the B pattern group (light blue), no gene expression was detected. Conversely, in the
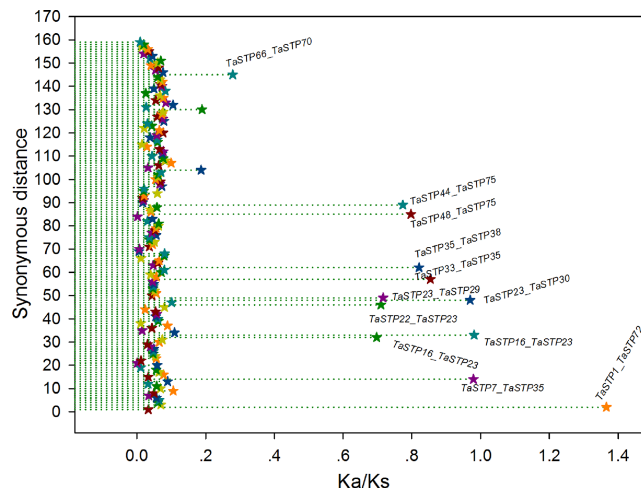
Figure 9 **The Ka/Ks ratios of the gene pairs in the duplication blocks.** The *x*- and *y*-axes denote the Ka/Ks ratio and the synonymous distance for each gene pair, respectively. The Ka/Ks values are presented by the star symbol.

Full-size 🖾 DOI: 10.7717/peerj.11371/fig-9

C pattern group (pale red), most genes, such as *TaSTP27* and *TaSTP48,* in the different tissues showed positively-regulated expression and, specifically, a higher expression level in the flag leaf blades and roots. Some genes were highly expressed in the seed coat, such as *TaSTP52, TaSTP53, TaSTP60, TaSTP61, TaSTP65,* and *TaSTP6 6*. In the stressed seedling leaves, the expression pattern was roughly divided into two groups: one group showed negative regulation with low expression compared with that of the control, such as the expression patterns in heat, drought stress or heat and drought combined stress at one hour and six hours, and the other group was positively or negatively regulated by PEG6000 stress at two hours and 12 h in nine-day-old seedlings of Giza168 and Gemmiza 10. Furthermore, compared with the gene expression in the no stress control, most genes were upregulated in shoots under cold stress at 4 °C for two weeks, except for the genes *TaSTP44, TaSTP* 53, *TaSTP56,* and *TaSTP61* (Fig. S1).

Bioinformatic-based protein interaction network analysis of the TaSTPs using STRING 10.5 and GO analyses

To explore the relationship between all the identified TaSTPs, we created a protein interaction network by searching the 81 proteins against the TAIR (The *Arabidopsis* Information Resource) database in STRING. We found 17 proteins with hits in the STRING database. These proteins interactions were divided into three groups: the first group (blue) was transglycosidase (DIN10), which is involved in the synthesis of raffinose, a major soluble carbohydrate in seeds, roots and tubers, and the second group (green) was trehalose phosphate synthase and trehalose-6-phosphate phosphatase (which removes the phosphate from trehalose 6-phosphate to produce free trehalose that accumulates in plants and may improve abiotic stress tolerance). The third group (red) was beta-fructofuranosidase (ATBFRUCT1, that can use sucrose and 1-kestose), glutamate synthase, and glutamate dehydrogenase, which are required during photorespiration (Fig. S2).
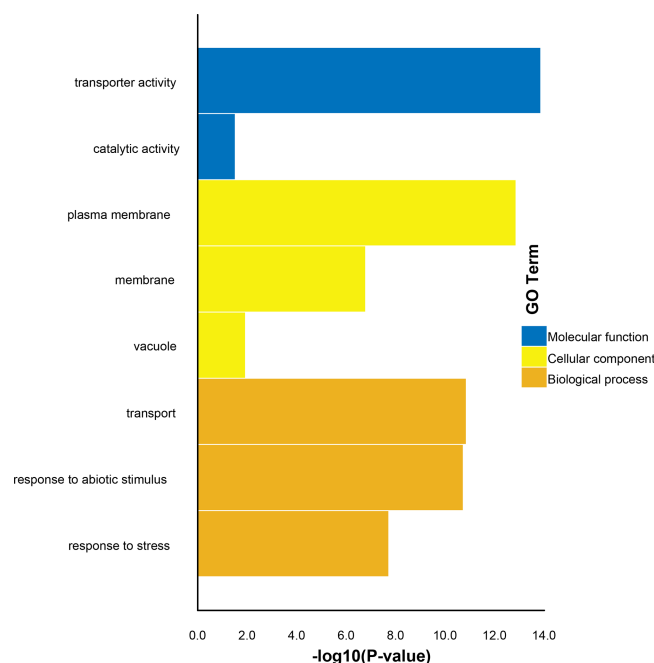
Figure 10 **Enrichment of GO terms in the three main categories for the 81 TaSTP genes considered in this study.** Three main categories, namely, molecular function, cellular component and biological process, are shown in blue terms, bright yellow terms, and brownish yellow terms, respectively.

Full-size ⬜ DOI: 10.7717/peerj.11371/fig-10

To further identify the functions of the putative TaSTP proteins in wheat, molecular functions, cellular components, and biological pathway categories were predicted using GO annotation analysis. Based on amino acid similarity, the results of the GO analysis showed that 81 TaSTP proteins were categorized into eight functional categories (Fig. 10). Among the molecular functions, transporter activity and catalytic activity were predominant. The analysis of the cellular component annotations revealed that most of the TaSTP proteins were predominantly localized to the plasma membrane, membrane and vacuole. Furthermore, 81 TaSTP proteins were assigned to transport, response to abiotic stimulus, and response to stress based on biological process analyses.

## Phenotype comparison of seedling roots, stems, and leaves under stress

Stress treatment was performed when seedlings grew to the second-true leaf stage. Wheat seedlings were divided into four groups with 100 seedlings per group and were treated with 150 mmol L^{-1}NaCl, 10% PEG6000 solution, 10% PEG6000 solution+150 mmol L^{-1}NaCl, or the control. Investigations were carried out after three, six, and nine days of stress, and the length and width of the roots, stems and leaves were accurately measured using vernier callipers. The phenotypes of the seedling roots, stems, and leaves under stress were different from those of the normal seedlings, and the most obvious difference was in root length (Figs. S3A–S3L). Specifically, at the three time points of stress, the root length of control was slightly elongated, while NaCl stress and PEG6000+NaCl stress did not change

Liu et al. (2021), *PeerJ*, DOI 10.7717/peerj.11371

16/26

significantly in the root length. Interestingly, the root lengths of plants under PEG6000 stress continued to increase and were significantly different from that of the control on the sixth day and ninth day of stress ($P < 0.01$) (Fig. S4A). In contrast, the root width of the control, NaCl stress, and PEG6000+NaCl stress plants gradually decreased as the plants grew. The root width of PEG6000 tended to be thinner on the sixth day and then thicker on the ninth day, but it was significantly thinner than that of the control (Fig. S4B). In the stems, there was no significant change in length among the four types of seedlings, but the diameter of the seedlings treated with stress was thinner than that of the control on the sixth and ninth days of treatment and showed significant ($P < 0.05$) or extremely significant ($P < 0.01$) differences. (Figs. S4C and S4D). The lengths of first true leaves of control were slightly shorter than those of the stressed leaves, but the width was wider than that of the stressed leaves (Figs. S4E and S4F). The length and width of the second true leaves of the NaCl-stressed and PEG6000+NaCl-stressed seedlings were significantly shorter than those of the control leaves ($P < 0.01$). However, the PEG6000-stressed leaves had approximately the same length and width as the control leaves (Figs. S4G and S4H).

Expression characteristics of wheat *TaSTP* genes using qRT-PCR analysis

We investigated the expression levels of the *TaSTP* genes during stress at the sixth day of wheat development to further explore *TaSTP* gene functions in wheat. First, we randomly selected four genes, *TaSTP12, TaSTP41, TaSTP48,* and *TaSTP65,* for qRT-PCR analysis, and their expression is quantified in Fig. 11. The results showed that these genes were expressed in the roots, stems, and leaves. Interestingly, the expression levels of the individual genes in the leaves were not the same but the expression of the same genes in the leaves was not affected by stress. For the gene *TaSTP 12,* the expression levels in the stressed wheat stems were similar but they were lower than those in the control stems; the difference was significant ($P < 0.05$). The expression of *TaSTP 12* was significantly higher in the stressed roots than in the control roots, and the differences were extremely significant, with a 1.4-fold change and 2.11-fold change in the roots of the NaCl-stressed and PEG6000+NaCl-stressed roots, respectively ($P < 0.01$) (Fig. 11A). Compared with *TaSTP 41* expression in the control stems, *TaSTP 41* expression was significantly downregulated in the PEG6000+NaCl-stressed (2.17-fold change, $P < 0.01$) and PEG6000-stressed stems (1.18-fold change, $P < 0.01$), but the NaCl-stressed did not show a difference. *TaSTP 41* expression was significantly upregulated in the PEG6000+NaCl-stressed (1.16-fold change, $P < 0.01$) and NaCl-stressed (1.4-fold change, $P < 0.01$) roots relative to the control roots. However, the expression was significantly downregulated (1.26-fold change, $P < 0.01$) in the PEG6000-stressed roots relative to the control roots (Fig. 11B). A difference in expression was not detected for the gene *TaSTP 48* between the control stems and stressed stems. In the roots, the expression level of *TaSTP 48* increased in the stressed roots compared with that in the control roots, and this was especially the case with PEG6000 stress, which showed more than a 10.04-fold change ($P < 0.01$) (Fig. 11C). *TaSTP 65* expression was significantly downregulated in the PEG6000+NaCl-stressed (8.62-fold change, $P < 0.01$) and NaCl-stressed (7.07-fold change, $P < 0.01$) stems compared with
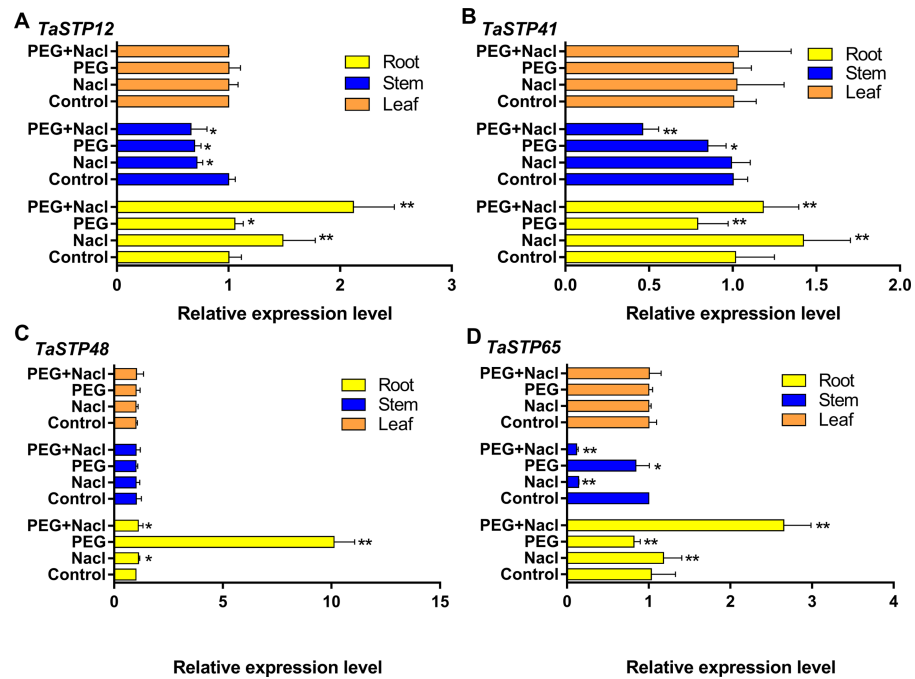
Figure 11 Comparison of the relative expression levels of four TaSTPs involved in different tissues on sixth day of the stress treatments. The x-axes indicate the relative gene expression levels; the y-axes indicate the different stress treatments in the root, stem and leaf tissues. A to D show the relative expression level of *TaSTP 12, TaSTP 41, TaSTP 48* and *TaSTP 65* genes in root, stem and leaf under NaCl stress, PEG6000 stress and their combined stresses and the control after 6 days, respectively. Capped lines indicate standard error. * $P < 0.05$; ** $P < 0.01$.

that in the control stems. In the roots, significantly elevated expression levels were seen with sodium chloride stress, specifically, a 1.15-fold change and a 2.57-fold change with NaCl stress and PEG6000+NaCl stress, respectively, ($P < 0.01$). Moreover, *TaSTP 65* showed a lower expression with a 1.26-fold change ($P < 0.01$) in the PEG6000-stressed roots compared to that in the control roots (Fig. 11D).

DISCUSSION

A large number of studies have shown that plants suffering from drought or salt stress can significantly increase their soluble sugar content, and soluble sugar is mainly involved in osmotic adjustment within the cell. The soluble sugar content is significantly positively correlated with plant stress and can be used as a screening index for stress resistance (*Gupta & Kaur, 2006*; *Rizhsky et al., 2004*). Furthermore, recent studies have shown that glucose and sucrose are important regulators of plant growth and gene expression, with hormone-like primary messenger functions, and participate in the regulation of plant growth and development under biotic and abiotic stress (*Rolland, Baena-Gonzalez & Sheen, 2006*). The most important function of sugar transporters is their role in mediating the long-distance transport of sugars in the phloem during plant development. STP genes have been cloned from various plants and organs, such as *Arabidopsis* and sorghum,

and food crops, including rice, barley, maize. However, 14 STP genes were found in *Arabidopsis*, which has a relatively small genome (125 Mb), so there are certainly many STP genes waiting to be discovered in the large wheat genome (17 Gb). We globally analysed the gene structure, protein motifs and phylogenetic tree of the TaSTP family in wheat for the first time. Furthermore, we investigated the expression of the TaSTP genes in different tissues during stress at sixth day of wheat development using qRT-PCR analysis to deeply explore TaSTP gene functions.

Eighty-one TaSTP genes were identified in the wheat genome through a BLAST search and HMMER analysis (Table 1), and they were distributed in the A, B, and D genomes. MEME results showed that most of the genes contained 12–13 motifs, and some were missing one or several motifs, indicating that the loss of the N-terminal or C-terminal regions may have occurred in some TaSTP members during evolution (Fig. 3). These results were in agreement with those obtained by studies in tomato, grape, and cassava (*Liu et al., 2018b*; *Reuscher et al., 2014*). The result of phylogenetic analysis showed that 81 TaSTPs, together with other STP proteins from wheat, *Brachypodium distachyon*, foxtail millet, rice, *Arabidopsis*, cassava, and *Ricinus communis* were classified into five groups and that the cloned wheat STP genes were in the same broad category as the TaSTP members we identified. Therefore, a close relationship between the cloned wheat STP proteins and TaSTP members indicated that these proteins possibly possess similar biochemical properties. Additionally, the RNA-seq data from seventeen tissues indicated that the TaSTP genes are differentially expressed in various tissues. Moreover, responses to abiotic stimuli and responses to stress were shown from the results of the biological process analysis of GO annotation. These results indicated that sucrose transporters are closely related to stress.

Thus, based on the phenotype comparisons, qRT-PCR was performed for the stressed wheat seedlings. Interestingly, the expression levels of the individual genes were different in the leaves, but the expression levels of the same genes were basically not affected by stress in the leaves (Fig. 11). Our findings also indicated that the expression of the sugar transporter gene in leaves may not be affected by short-term stress processes. The pattern of STP expression in the wheat stems subjected to stress differed from that in the leaves. The expression pattern of the TaSTP genes was downregulated in stressed plants compared with that in the control plants. Among them, *TaSTP12* was significantly downregulated under the three stress patterns. *TaSTP41* showed no significant downregulation under NaCl stress but showed significant downregulation under PEG-related stress. *TaSTP48* did not show significant differences, but there was slight trend for downregulation. *TaSTP65* showed significant downregulation in all stressed stems, and it showed an extremely significant downward trend under NaCl-related stress. These results are in agreement with those obtained from cold-stressed seedling stems from the RNA-seq data from the website (*TaSTP12 ,48,65*). These results may be related to the thin and short stems that grew under stress. Some genes have a clear propensity for stress response and the *TaSTP65* gene may be closely related to NaCl stress in the stems. It has been shown that STP expression does not always correspond to phloem unloading, and consistent patterns of STP expression under stress indicate which types of STPs are involved in stress tolerance (*Truernit et al., 1996*; *Julius et al., 2017*).

In our study, the most striking change was observed in STP genes in the roots and *STP 13* expression was markedly increased in the roots after NaCl treatment in *Arabidopsis* (*Yamada et al., 2011*). The expression of *TaSTP12*, *41*, *48*, and *65* was significantly or extremely significantly upregulated in the roots under NaCl-related stress compared to that under the control treatment. However, the STP gene exhibited two opposite expression trends in the roots when PEG6000 was involved in the stress. The *TaSTP41* and *TaSTP65* genes were extremely significantly downregulated, while the *TaSTP12* and *TaSTP48* genes were significant upregulated. Among these four genes, the expression abundance of *TaSTP48* was upregulated up to ten times higher than that in the control, and the other three expression abundances were lower (Fig. 11). Thus, we speculate that *TaSTP48* plays a key role in PEG6000 stress in roots. In *Arabidopsis,* it has been reported that a stress-induced monosaccharide transporter gene, *ESL1,* may cooperate with the sucrose invertase gene in the tonoplast to affect the accumulation of intracellular sugars, thereby regulating the response of plants to abiotic stress (*Yamada et al., 2010*). According to the latest research, it has been reported that the overexpression of *DsSWEET17* in *Arabidopsis* confers tolerance to salt and oxidative stresses (*Zhou et al., 2018*). Furthermore, the sugar transporter gene *ERD6* could be upregulated by drought and salt stress in maize (*Ma et al., 2009*). Drought and high salinity stresses significantly induced the upregulation of *STP13* in *Arabidopsis.* Thus, we speculate that the high expression of *STP13* in the cortex and endodermis may be related to the reabsorption of monosaccharides released from damaged epidermal cells. These findings suggest that the *STP13* gene is involved in an adaptive response to increase cell osmotic pressure or to reduce nutrient loss under abiotic stress (*Yamada et al., 2011*). Moreover, the proteomics of osmotic stress indicated that water-soluble carbohydrates, including glucose and fructose, were increased in the roots, stems, and leaves in stress plants compared with normal wheat (*Ma et al., 2016*). Therefore, these results suggest that the *TaSTP* gene may be vital to monosaccharide distribution, regulating the seedling stem and root growth of wheat under drought or salt stress, which is a hypothesis that merits further study.

CONCLUSION

We analyzed the sugar transporter genes of wheat at the genome level. Eighty-one TaSTP genes were identified. Gene structure, protein motifs, GO analyses, the expression pattern indicate the conservative and diversified nature of TaSTP genes. Synteny analysis and phylogenetic comparison of TaSTP genes from several different plant species provided valuable insight on the evolutionary characteristics of wheat TaSTP genes. Phylogenetic and gene expression analyses provided important information for the functional analysis of *TaSTP* genes. Our study is a valuable resource for the better understanding of the biological roles of individual TaSTP genes in wheat.

ADDITIONAL INFORMATION AND DECLARATIONS

Competing Interests

The authors declare there are no competing interests.

Author Contributions

- Hongzhan Liu conceived and designed the experiments, performed the experiments, analyzed the data, prepared figures and/or tables, authored or reviewed drafts of the paper, and approved the final draft.
- Chaoqiong Li and Xueqin Wang analyzed the data, prepared figures and/or tables, contributed reagents/materials/analysis tools, and approved the final draft.
- Lin Qiao, Junsheng Wang and Xianle Ruan analyzed the data, authored or reviewed drafts of the paper, contributed reagents/materials/analysis tools, and approved the final draft.
- Lizong Hu performed the experiments, prepared figures and/or tables, and approved the final draft.
- Guangyu Yang analyzed the data, prepared figures and/or tables, and approved the final draft.

- Guihong Yin conceived and designed the experiments, authored or reviewed drafts of the paper, contributed reagents/materials/analysis tools, and approved the final draft.
- Chunping Wang, Zhongke Sun and Keshi Ma analyzed the data, authored or reviewed drafts of the paper, contributed reagents/materials/analysis tools, and approved the final draft.
- Lili Li conceived and designed the experiments, authored or reviewed drafts of the paper, contributed reagents/materials/analysis tools, and approved the final draft.

Data Availability

The following information was supplied regarding data availability:

The raw data are available in the Supplementary Files.

Supplemental Information

Supplemental information for this article can be found online at http://dx.doi.org/10.7717/peerj.11371#supplemental-information.

REFERENCES

Afoufa-Bastien D, Medici A, Jeauffre J, Coutos-Thévenot P, Lemoine R, Atanassova R, Laloi M. 2010. The Vitis vinifera sugar transporter gene family: phylogenetic overview and macroarray expression profiling. *BMC Plant Biology* **10**:245 DOI 10.1186/1471-2229-10-245.

Balibrea Lara ME, Gonzalez Garcia MC, Fatima T, Ehness R, Lee TK, Proels R, Tanner W, Roitsch T. 2004. Extracellular invertase is an essential component of cytokinin-mediated delay of senescence. *The Plant Cell* **16**(5):1276–1287 DOI 10.1105/tpc.018929.

Braun DM, Slewinski TL. 2009. Genetic control of carbon partitioning in grasses: roles of sucrose transporters and tie-dyed loci in phloem loading. *Plant Physiology* **149**(1):71–81 DOI 10.1104/pp.108.129049.

Brenchley R, Spannagl M, Pfeifer M, Barker GLA, D'Amore R, Allen AM, Mckenzie N, Kramer M, Kerhornou A, Bolser DM, Suzanne Kay, Waite D, Trick M, Bancroft I, Gu YQ, Huo N, Luo M, Sehgal SK, Kianian S, Gill BS, Anderson OD, Kersey PJ, Dvořák J, McCombie RW, Hall A, Mayer KFX, Edwards KJ, Bevan MW, Hall N. 2012. Analysis of the bread wheat genome using whole-genome shotgun sequencing. *Nature* **491**:705–710 DOI 10.1038/nature11650.

Bush DR. 1993. Proton-coupled sugar and amino acid transporters in plants. *Annual Review of Plant Biology* **44**:513–542 DOI 10.1146/annurev.pp.44.060193.002501.

Bush DR. 1999. Sugar transporters in plant biology. *Current Opinion in Plant Biology* **2**:187–191 DOI 10.1016/S1369-5266(99)80034-X.

Büttner M. 2007. The monosaccharide transporter(-like) gene family in arabidopsis. *FEBS Letters* **581**(12):2318–2324 DOI 10.1016/j.febslet.2007.03.016.

Büttner M. 2010. The *Arabidopsis* sugar transporter (AtSTP) family: an update. *Plant Biology* **12**:35–41.

Cao Y, Han Y, Meng D, Li D, Jin Q, Lin Y, Cai Y. 2016. Structural, evolutionary, and functional analysis of the class III peroxidase gene family in Chinese pear (*Pyrus bretschneideri*). *Frontiers in Plant Science* **7**:1874.

Chen C, Xia R, Chen H, He Y. 2018. TBtools, a toolkit for biologists integrating various HTS-data handling tools with a user-friendly interface. *bioRxiv* 289660.

Djanaguiraman M, Prasad PVV, Kumari J, Rengel Z. 2019. Root length and root lipid composition contribute to drought tolerance of winter and spring wheat. *Plant and Soil* **439**:57–73 DOI 10.1007/s11104-018-3794-3.

Doidy J, Vidal U, Lemoine R. 2019. Sugar transporters in Fabaceae, featuring SUT MST and SWEET families of the model plant *Medicago truncatula* and the agricultural crop *Pisum sativum*. *PLOS ONE* **14(9)**:e0223173 DOI 10.1371/journal.pone.0223173.

Du YC, Nose A, Kondo A, Wasano K. 2000. Diurnal changes in photosynthesis in sugarcane leaves: II. Enzyme activities and metabolite levels relating to sucrose and starch metabolism. *Plant Production Science* **3(1)**:9–16 DOI 10.1626/pps.3.9.

Endler A, Meyer S, Schelbert S, Schneider T, Weschke W, Peters SW, Keller F, Baginsky S, Martinoia E, Schmidt UG. 2006. Identification of a vacuolar sucrose transporter in barley and *Arabidopsis* mesophyll cells by a tonoplast proteomic approach. *Plant Physiology* **141**:196–207 DOI 10.1104/pp.106.079533.

Finn RD, Mistry J, Tate J, Coggill P, Heger A, Pollington JE, Gavin OL, Gunasekaran P, Ceric G, Forslund K, Holm L, Sonnhammer ELL, Eddy SR, Bateman A. 2010. The Pfam protein families database. *Nucleic Acids Research* **38**:D211–D222 DOI 10.1093/nar/gkp985.

Fotopoulos V, Gilbert MJ, Pittman JK, Marvier AC, Buchanan AJ, Sauer N, Hall JL, Williams LE. 2003. The monosaccharide transporter gene, AtSTP4, and the cell-wall invertase, At βfruct1, are induced in *Arabidopsis* during infection with the fungal biotroph Erysiphe cichoracearum. *Plant Physiology* **132**:821–829 DOI 10.1104/pp.103.021428.

Gupta AK, Kaur N. 2006. Sugar signalling and gene expression in relation to carbohydrate metabolism under abiotic stresses in plants. *Journal of Biosciences* **30**:761–776.

Hedrich R, Sauer N, Neuhaus HE. 2015. Sugar transport across the plant vacuolar membrane: nature and regulation of carrier proteins. *Current Opinion in Plant Biology* **25**:63–70 DOI 10.1016/j.pbi.2015.04.008.

Johnson DA, Thomas MA. 2007. The monosaccharide transporter gene family in Arabidopsis and rice: a history of duplications, adaptive evolution, and functional divergence. *Molecular Biology & Evolution* **24**:2412–2423 DOI 10.1093/molbev/msm184.

Julius BT, Leach KA, Tran TM, Mertz RA, Braun DM. 2017. Sugar transporters in plants: new insights and discoveries. *Plant and Cell Physiology* **58**:1442–1460 DOI 10.1093/pcp/pcx090.

Kong W, An B, Zhang Y, Yang J, Li S, Sun T, Li Y. 2019. Sugar transporter proteins (STPs) in gramineae crops: comparative analysis, phylogeny, pvolution, and expression profiling. *Cell* **8(6)**:Article 560 DOI 10.3390/cells8060560.

Krzywinski M, Schein JI, Birol I, Connors J, Gascoyne R, Horsman D, Jones SJ, Marra MA. 2009. Circos: an information aesthetic for comparative genomics. *Genome Research* **19**:1639–1645 DOI 10.1101/gr.092759.109.

Kumar S, Stecher G, Tamura K. 2016. MEGA7: molecular evolutionary genetics analysis version 7.0 for bigger datasets. *Molecular Biology & Evolution* **33**:1870–1874 DOI 10.1093/molbev/msw054.

Lastdrager J, Hanson J, Smeekens S. 2014. Sugar signals and the control of plant growth and development. *Journal of Experimental Botany* **65**:799–807 DOI 10.1093/jxb/ert474.

Letunic I, Bork P. 2018. 20 years of the SMART protein domain annotation resource. *Nucleic Acids Research* **46**:D493–D496 DOI 10.1093/nar/gkx922.

Li J, Zheng D, Li L, Qiao X, Wei S, Bai B, Zhang S, Wu J. 2015. Genome-wide function, evolutionary characterization and expression analysis of sugar transporter family genes in Pear (*Pyrus bretschneideri* Rehd). *Plant & Cell Physiology* **56(9)**:1721–1737 DOI 10.1093/pcp/pcv090.

Liu H, Wang J, Li C, Lin Q, Wang X, Li J, Hu L, Yin G, Ba Q. 2018a. Phenotype characterisation and analysis of expression patterns of genes related mainly to carbohydrate metabolism and sporopollenin in male-sterile anthers induced by high temperature in wheat (*Triticum aestivum*). *Crop & Pasture Science* **69**:469–478 DOI 10.1071/CP18034.

Liu Q, Dang H, Chen Z, Wu J, Chen Y, Chen S, Luo L. 2018b. Genome-wide identification, expression, and functional analysis of the sugar transporter gene family in Cassava (*Manihot esculenta*). *International Journal of Molecular Sciences* **19**:Article 987 DOI 10.3390/ijms19040987.

Ludewig F, Flügge UI. 2013. Role of metabolite transporters in source–sink carbon allocation. *Frontiers in Plant Science* **4**:Article 231.

Ma J, Dong W, Zhang D, Gao X, Jiang L, Shao Y, Tong D, Li X. 2016. Proteomic profiling analysis reveals that glutathione system plays important roles responding to osmotic stress in wheat (*Triticum aestivum L.*) roots. *Peerj* **4**:e2334 DOI 10.7717/peerj.2334.

Ma X, Liu Y, Yuan Z, Shi Y, Song Y, Wang T, Li Y. 2009. Cloning of cDNAs for a novel sugar transporter gene, ZmERD6, from maize and its expression analysis under abiotic stresses. *Acta Agronomica Sinica* **35**:1410–1417 DOI 10.3724/SP.J.1006.2009.01410.

Mathieu AS, Tinel C, Dailly H, Quinet M, Lutts S. 2018. Impact of high temperature on sucrose translocation, sugar content and inulin yield in *Cichorium intybus* L. var. sativum. *Plant and Soil* **432**:273–288 DOI 10.1007/s11104-018-3802-7.

Paulsen PA, Custódio TF, Pedersen BP. 2019. Crystal structure of the plant symporter STP10 illuminates sugar uptake mechanism in monosaccharide transporter superfamily. *Nature Communications* **10**:Article 407 DOI 10.1038/s41467-018-08176-9.

Reuscher S, Akiyama M, Yasuda T, Makino H, Aoki K, Shibata D, Shiratake K. 2014. The sugar transporter inventory of tomato: genome-wide identification and

expression analysis. *Plant & Cell Physiology* **55**:1123–1141
DOI 10.1093/pcp/pcu052.

Rizhsky L, Liang H, Shuman J, Shulaev V, Davletova S, Mittler R. 2004. When defense pathways collide. The response of *Arabidopsis* to a combination of drought and heat stress. *Plant Physiology* **134**:1683–1696 DOI 10.1104/pp.103.033431.

Roitsch T, González M. 2004. Function and regulation of plant invertases: sweet sensations. *Trends in Plant Science* **9**(12):606–613
DOI 10.1016/j.tplants.2004.10.009.

Rolland F, Baena-Gonzalez E, Sheen J. 2006. Sugar sensing and signaling in plants: conserved and novel mechanisms. *Annual Review of Plant Biology* **57**:675–709
DOI 10.1146/annurev.arplant.57.032905.105441.

Rottmann T, Klebl F, Schneider S, Kischka D, Rüscher D, Sauer N, Stadler R. 2018. Sugar transporter STP7 specificity for L-arabinose and D-xylose contrasts with the typical hexose transporters STP8 and STP12. *Plant Physiology* **176**:2330–2350
DOI 10.1104/pp.17.01493.

Sauer N, Tanner W. 1989. The hexose carrier from Chlorella. *FEBS Letters* **259**(1):43–46
DOI 10.1016/0014-5793(89)81489-9.

Schneidereit A, Scholz-Starke J, Büttner M. 2003. Functional characterization and expression analyses of the glucose-specific *AtSTP9* monosaccharide transporter in pollen of *Arabidopsis*. *Plant Physiology* **133**:182–190
DOI 10.1104/pp.103.026674.

Schneidereit A, Scholz-Starke J, Sauer N, Büttner M. 2005. AtSTP11, a pollen tube-specific monosaccharide transporter in *Arabidopsis*. *Planta* **221**:48–55
DOI 10.1007/s00425-004-1420-5.

Schofield RA, Bi YM, Kant S, Rothstein SJ. 2009. Over-expression of STP13, a hexose transporter, improves plant growth and nitrogen use in *Arabidopsis thaliana* seedlings. *Plant, Cell & Environment* **32**(3):271–285
DOI 10.1111/j.1365-3040.2008.01919.x.

Scholz-Starke J, Büttner M, Sauer N. 2003. AtSTP6, a new pollen-specific H^+-monosaccharide symporter from *Arabidopsis*. *Plant Physiology* **131**:70–77
DOI 10.1104/pp.012666.

Sherson SM, Hemmann G, Wallace G, Forbes S, Germain V, Stadler R, Bechtold N, Sauer N, Smith SM. 2010. Monosaccharide/proton symporter AtSTP1 plays a major role in uptake and response of Arabidopsis seeds and seedlings to sugars. *Plant Journal* **24**:849–857.

Slewinski TL, Meeley R, Braun DM. 2009. Sucrose transporter1 functions in phloem loading in maize leaves. *Journal of Experimental Botany* **60**:881–892
DOI 10.1093/jxb/ern335.

Truernit E, Schmid J, Epple P, Illig J, Sauer N. 1996. The sink-specific and stress-regulated Arabidopsis STP4 gene: Enhanced expression of a gene encoding a monosaccharide transporter by wounding, elicitors, and pathogen challenge. *The Plant Cell* **8**:2169–2182.

Yamada K, Kanai M, Osakabe Y, Ohiraki H, Shinozaki K, Yamaguchi-Shinozaki K. 2011. Monosaccharide absorption activity of Arabidopsis roots depends on expression profiles of transporter genes under high salinity conditions. *Journal of Biological Chemistry* **286**(50):43577–43586 DOI 10.1074/jbc.M111.269712.

Yamada K, Osakabe Y, Mizoi J, Nakashima K, Fujita Y, Shinozaki K, Yamaguchi-Shinozaki K. 2010. Functional analysis of an *Arabidopsis thaliana* abiotic stress-inducible facilitated diffusion transporter for monosaccharides. *Journal of Biological Chemistry* **285**:1138–1146 DOI 10.1074/jbc.M109.054288.

Yan N. 2013. Structural advances for the major facilitator superfamily (MFS) transporters. *Trends in Biochemical Sciences* **38**(3):151–159 DOI 10.1016/j.tibs.2013.01.003.

Yue W, Nie X, Cui L, Zhi Y, Zhang T, Du X, Song W. 2018. Genome-wide sequence and expressional analysis of autophagy gene family in bread wheat (*Triticum aestivum* L.). *Journal of Plant Physiology* **229**:7–21 DOI 10.1016/j.jplph.2018.06.012.

Zhang L, Zhang C, Yang B, Xiao Z, Ma J, Liu J, Jian H, Qu C, Lu K, Li J. 2020. Genome-wide identification and expression profiling of monosaccharide transporter genes associated with high harvest index values in rapeseed (*Brassica napus* L.). *Gene* **11**(6):Article 653 DOI 10.3390/genes11060653.

Zhang Y, Zhang DB, Liu M. 2015. The molecular mechanism of long-distance sugar transport in plants. *Chinese Bulletin of Botany* **50**(1):107–121 DOI 10.3724/SP.J.1259.2015.00107.

Zheng QM, Tang Z, Xu Q, Deng XX. 2014. Isolation, phylogenetic relationship and expression profiling of sugar transporter genes in sweet orange (*Citrus sinensis*). *Plant Cell Tissue & Organ Culture* **119**:609–624 DOI 10.1007/s11240-014-0560-y.

Zhou A, Ma H, Feng S, Gong S, Wang J. 2018. DsSWEET17, a tonoplast-localized sugar transporter from dianthus spiculifolius, affects sugar metabolism and confers multiple stress tolerance in *Arabidopsis*. *International Journal of Molecular Sciences* **19**:Article 1564 DOI 10.3390/ijms19061564.